HAMAMATSU
PHOTON IS OUR BUSINESS

FTIR engine (FT-NIR spectrometer)

Contents

1. Overview

The Fourier transform infrared spectrometer (FTIR) engine is compact enough to carry in just one hand. A Michelson optical interferometer and control circuit are built into a palm-sized enclosure. Spectrum and absorbance can be measured by connecting a PC via USB. It can be applied to real-time measurement performed on site without bringing the measurement sample into the analysis room as well as continuous monitoring.
The FTIR engine's optical interferometer has a movable mirror (ϕ3 mm) that uses Micro Electro Mechanical Systems (MEMS) technology and a fixed mirror. The built-in semiconductor laser (VCSEL: vertical cavity surface emitting laser) for monitoring the movable mirror position allows spectrum measurement with high wavelength accuracy. The product includes evaluation software with functions for setting measurement conditions, acquiring and saving data, drawing graphs, and so on. Furthermore, the dynamic link library (DLL) function specifications are disclosed, so users can create their original measurement software programs.

2. Structure

The FTIR has the following features compared to the dispersive type (diffraction grating type) spectrometer.

- High S/N because simultaneous signal measurements are possible in the entire spectral range
- High light utilization efficiency if the resolution is the same as the dispersive type spectrometer since the incident hole can be enlarged
- High wavelength accuracy and reproducibility because laser wavelength is used for calibration

The FTIR's optical interferometer is composed of a light input section, beam splitter (semi-transparent mirror), fixed mirror, ϕ3 mm movable mirror, photodetector, and so on. The incident light is split into two light beams, transmitted light and reflected light, by a beam splitter. The two light beams are reflected by the fixed mirror and movable mirror and return to the beam splitter, where they are recombined, causing optical interference. The photodetector acquires light intensity signals that varies depending on the movable mirror position. The optical spectrum is obtained by taking the Fourier transform of this light intensity signal.

An optical fiber is connected to the connector at the light input section of the FTIR engine. Light from the measurement sample can be input to the FTIR engine through an optical fiber, which provides a highly flexible measurement system.

[Figure 2-1] FTIR configuration and operating principle

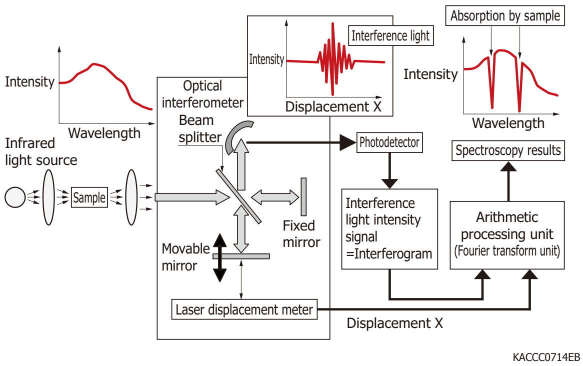

2 - 1 Movable mirror

The FTIR engine has a built-in electrostatically driven movable mirror [Figure 2-2]. When a voltage is applied to the comb electrodes, an electrostatic driving force is generated. As a result, the torsion bars twist causing the beams to move, and the movable mirror moves vertically in parallel. The movable mirror moves by a great amount when driven at the resonant frequency.

[Figure 2-2] Movable mirror and electrostatic actuator

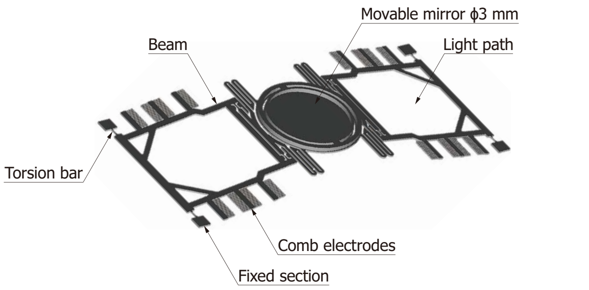

2 - 2 Optical interferometers

[Figure 2-3] (a) shows a typical interferometer used in an FTIR, and [Figure 2-3] (b) shows the interferometer used in the FTIR engine. The optical interferometer is composed of a light input section, beam splitter, fixed mirror, movable mirror, photodetector, and so on. Using a wavelength dispersion compensator made of the same material as the beam splitter, a fixed mirror is formed on the back side. The optical interferometer is designed so that the optical path difference between the movable mirror side and fixed mirror side is zero at the position where the movable mirror has moved about 70 µm (thickness of the movable mirror) below the position of the movable mirror in [Figure 2-3] (b).

The optical interferometer has a built-in MEMS chip shown in [Figure 2-4]. The MEMS chip is resin-sealed in a package [Figure 2-5]. It prevents the entry of fine particles, but moisture is permeable. Make sure condensation does not form on the beam splitter, lens, or movable mirror, as condensation may degrade the characteristics.

[Figure 2-3] Optical interferometer

(a) FTIR interferometer

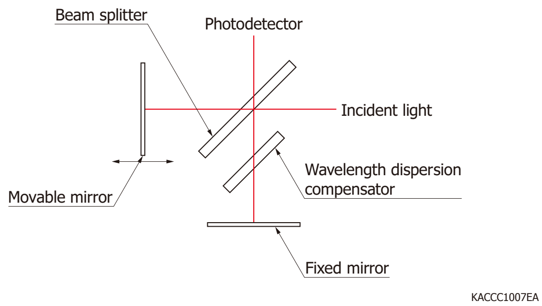

(b) FTIR engine interferometer

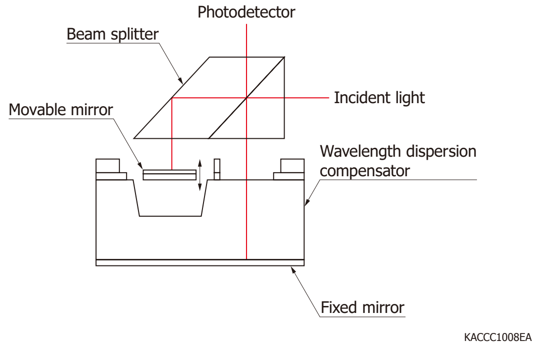

[Figure 2-4] MEMS chip (built into the optical interferometer)

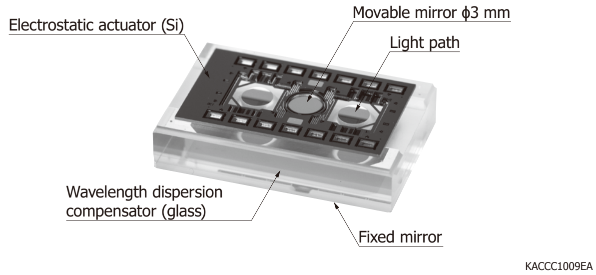

» Structure

[Figure 2-5] shows the optical system of the FTIR engine. There are two interferometers in the FTIR engine: infrared interferometer and laser interferometer. The infrared interferometer measures the near infrared light input from the optical fiber, and the laser interferometer monitors the movable mirror position using a semiconductor laser (VCSEL). The positions of the two optical interferometers are separated by a dichroic mirror. An InGaAs PIN photodiode (G12183-003K) is used for the infrared interferometer's photodetector and a Si PIN photodiode (S5821-03) for the laser interferometer's photodetector.

[Figure 2-5] Optical system of FTIR engine

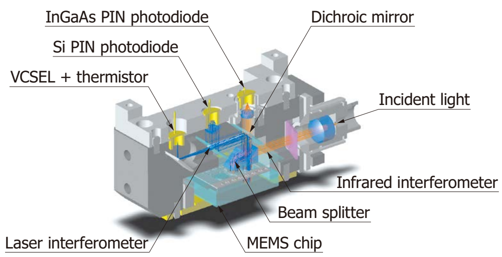

KACCC1010EA

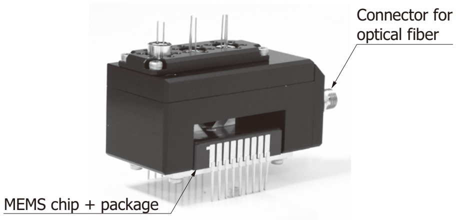

KACCC1011EA

2 - 3 Control circuit

The FTIR engine consists of four elements: an optical engine, an analog controller, a digital controller, and a communication controller. The optical signal detected by the optical engine is amplified by TIA (Transimpedance Amplifier) in the analog controller. The amplified optical signals are converted into digital signals by the A/D converter and sent to the digital controller. The FPGA (field-programmable gate array) located in the digital controller is used to set the analog controller, control the drive timing, and perform arithmetic processing. The calculated signal is transferred to the PC through the communication controller.

C15511-01

The C15511-01 connects to the PC via a USB interface. The controller of C15511-01 controller controls only the drive timing of the device. The optical signals obtained from the two photodetectors are transferred to the PC for spectrum operations including Fourier transforms in the PC.

[Figure 2-6] Block diagram (C15511-01)

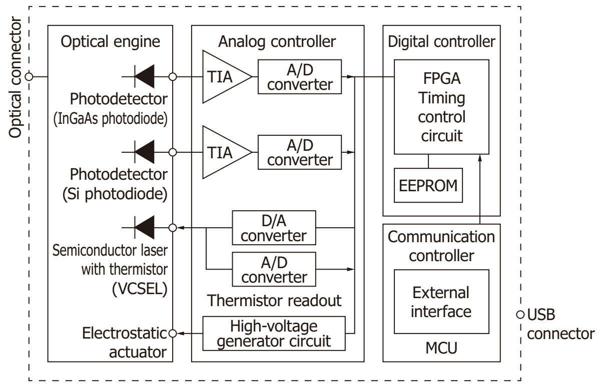

KACCC1012EB

C16511-01

The C16511-01 connects to the PC via an Ethernet interface. The controller of C16511-01 performs spectrum operations, including Fourier transforms, and transfers the spectral results to a PC. Operation is multithreaded for fast spectral measurement.

[Figure 2-7] Block diagram (C16511-01)

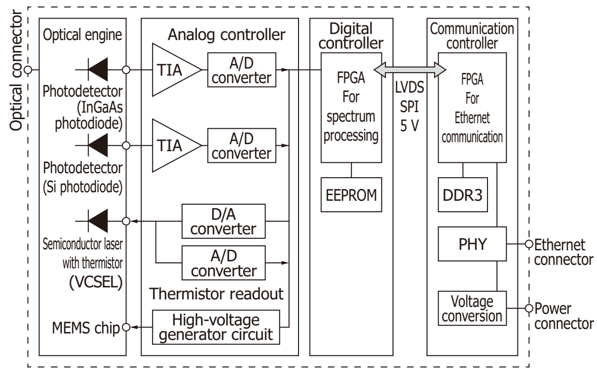

KACCC1235EA

2 - 4 Software

The FTIR engine comes with evaluation software to help you evaluate, Dynamic Link Library (DLL) to create your own measurement software, Software Development Kit (SDK), and drivers to connect the FTIR engine to your PC. The evaluation software allows you to set measurement conditions (gain, integration count, etc.), start measurement, view and save data graphically, etc. The SDK provides sample code for using DLL [Figure 2-8].

[Figure 2-8] Software configuration

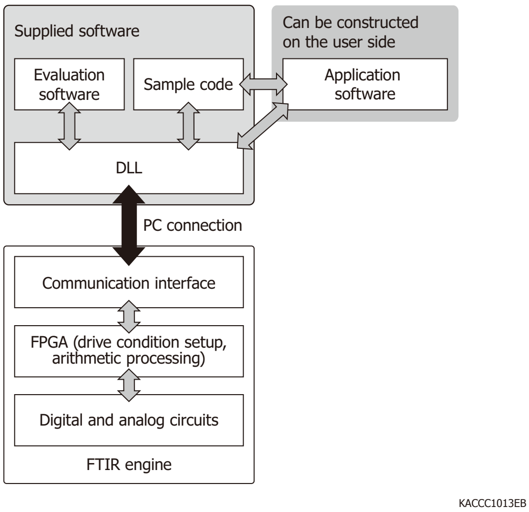

3. Operating principle

3 - 1 Movable mirror

The movable mirror drive conditions are stored in the EEPROM of the control circuit. The movable mirror can be driven in resonance by reading information from the EEPROM.

The electrostatic actuator that drives the movable mirror can be represented by the dynamic model in [Figure 3-1]. The spring constant is mainly determined by the Young's modulus and Poisson's ratio of the spring material and the spring shape (length, thickness, width). The spring is formed with high accuracy by applying semiconductor lithography technology and etching technology, but there are some variations in the spring dimensions and spring constant. Therefore, the drive frequency of the movable mirror varies by product.

[Table 3-1] Electrical characteristics (drive frequency) of movable mirror

Parameter	Min.	Typ.	Max.	Unit
Drive frequency	225	275	325	Hz

[Figure 3-1] Dynamic model of electrostatic actuator

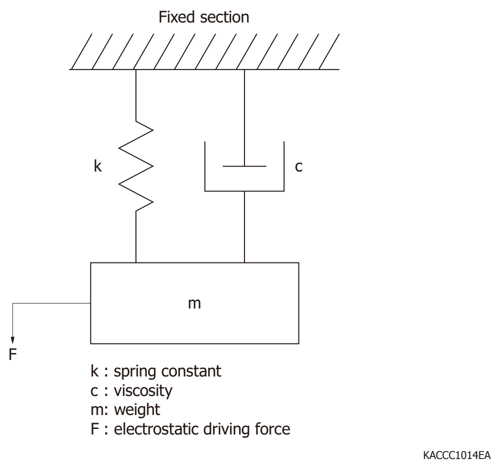

The spring characteristic of an electrostatic actuator has a non-linear characteristic called hardening, and the movable mirror's amplitude changes drastically at a specific drive frequency. This is shown by the duffing equation [Equation (3-1)]. In the range where the amplitude changes drastically, the characteristics differ from low frequency to high frequency and from high frequency to low frequency. In the range where the characteristics are the same, a stable amplitude can be obtained by setting the drive frequency [Figure 3-2].

$$m\ddot{x} + c\dot{x} + (1 + \beta x^2)kx = F\cos(wt) \quad \cdots\cdots\cdots\cdots\cdots \quad (3\text{-}1)$$

[Figure 3-2] Amplitude vs. drive frequency (typical example)

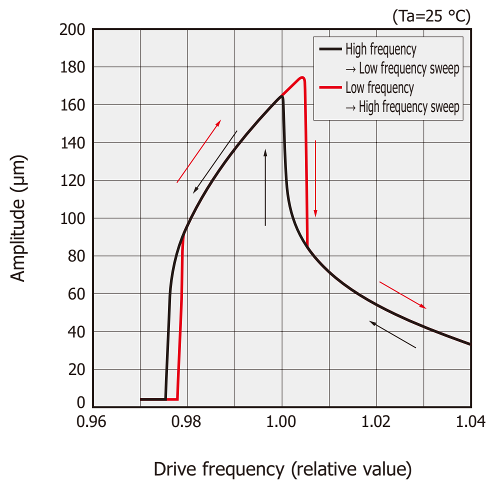

KACCB0594EA

The natural frequency of a movable mirror is expressed by [Equation (3-2)]. The resonant frequency of the movable mirror that has a non-linear spring shifts according to the amplitude [Equation (3-3)]. When the amplitude of the movable mirror increases due to hardening, the spring constant increases, which increases the resonant frequency [Figure 3-3].

$$\omega_0 = \sqrt{\frac{k}{m}} \quad \cdots\cdots\cdots\cdots\cdots \quad (3\text{-}2)$$

ω_0: natural frequency
m : weight
k : spring constant

$$\omega_1 = \omega_0 \sqrt{1 + \frac{3}{4}\beta x^2} \quad \cdots\cdots\cdots\cdots\cdots \quad (3\text{-}3)$$

ω_1: resonant frequency
β : non-linearity constant of spring
x : amplitude

The electrostatic driving force of the movable mirror is expressed by equation (3-4).

$$F = \frac{1}{2}\frac{dC}{dx}V^2 \quad \cdots\cdots\cdots\cdots\cdots \quad (3\text{-}4)$$

F: electrostatic driving force
C: capacitance of comb electrodes (composed of multiple parallel plates)
V: drive voltage

[Figure 3-3] Drive frequency characteristics (typical example)

(a) Amplitude vs. drive frequency

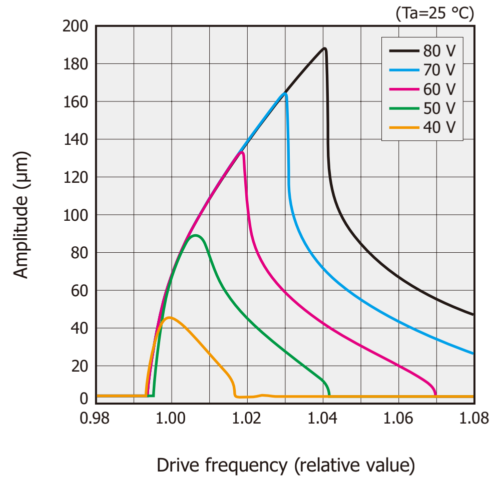

KACCB0595EA

(b) Maximum amplitude vs. drive frequency

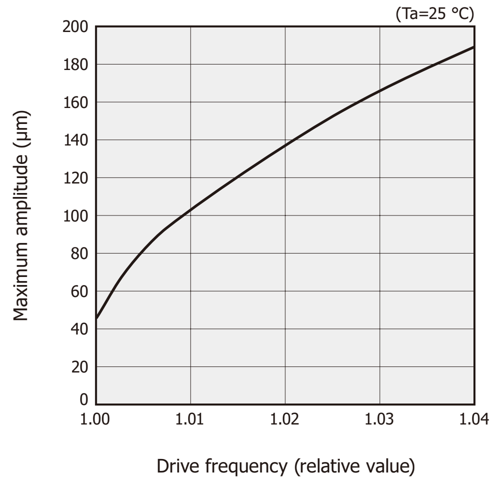

KACCB0596EA

Since the movable mirror spring is made of single-crystal silicon, it has the advantage of low metal fatigue and long life. As the temperature increases, the Young's modulus of the single-crystal silicon decreases. Therefore, when the temperature changes, the spring constant changes, which causes the movable mirror's resonant frequency to change [Figure 3-4].

[Figure 3-4] Temperature characteristics of drive frequency (typical example)

(a) Amplitude vs. drive frequency

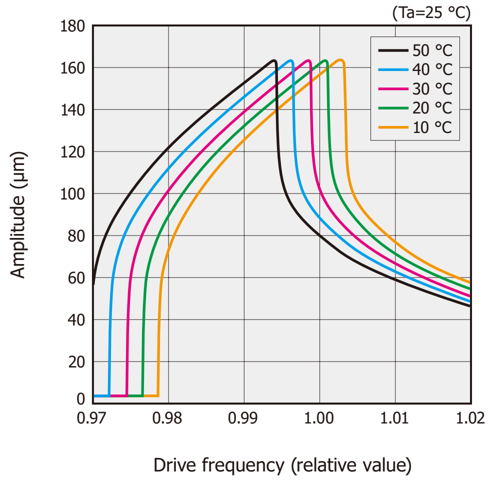

KACCB0597EA

(b) Drive frequency vs. ambient temperature

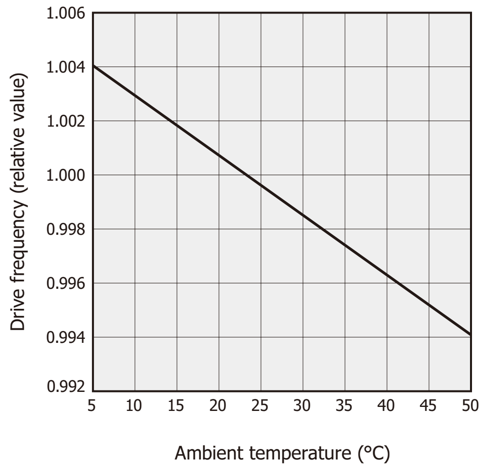

KACCB0598EA

Control method

The FTIR engine stores the optimum conditions in EEPROM in order to stably drive the movable mirror. In addition, the thermistor embedded in the FTIR engine enclosure measures the temperature, and the optimal drive frequency is set according to the temperature change. [Figure 3-5] shows the temperature characteristics of the movable mirror's drive frequency and amplitude.

[Figure 3-5] Temperature characteristics of drive frequency and amplitude (typical example)

(a) Drive frequency vs. temperature

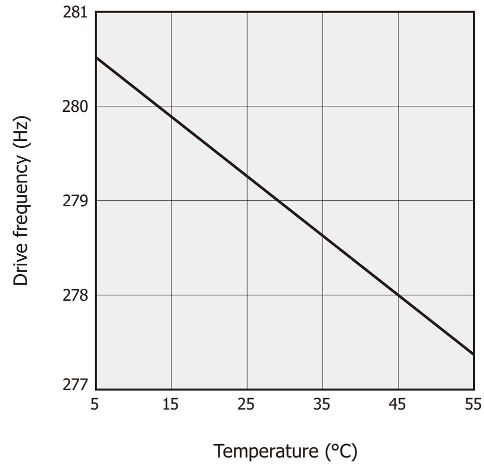

KACCB0599EA

(b) Amplitude vs. temperature

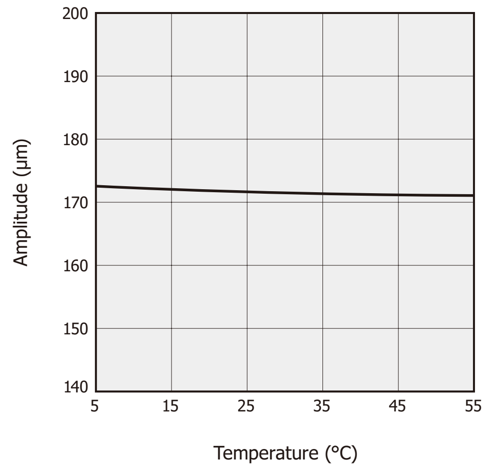

KACCB0600EA

3 - 2 Optical interferometers

The photocurrent obtained by inputting light to the optical interferometer (infrared interferometer, laser interferometer) is expressed by [Equation (3-5)]. The AC component in the second term of [Equation (3-5)] is an optical interference signal called an interferogram. At the position where the optical path difference between the movable mirror and fixed mirror is zero, the light of each wavelength interferes with each other, which increases the optical interference signal. As the distance from the zero optical path difference increases, the light of each wavelength interferes at various positions, which causes a decreasing ripple [Figure 3-6]. This optical interference signal can be Fourier transformed to obtain the optical spectrum.

$$I(x) = \int_0^{\infty} B(v)(1 + \cos 2\pi v x)dv \cdots\cdots\cdots\cdots (3\text{-}5)$$

I(x) : photocurrent
B(v): optical spectrum
V : wavenumber
X : optical path difference

[Figure 3-6] Optical interference signal

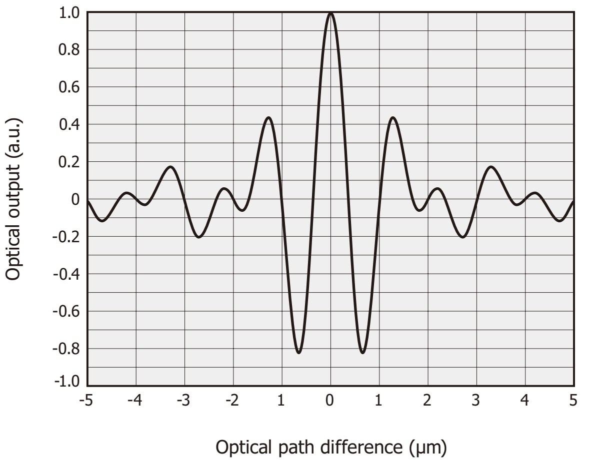

KACCB0601EA

The wavenumber resolution of the FTIR is defined by wavenumber Δv (unit: cm^{-1}), which is the reciprocal of the wavelength of light. The wavenumber resolution is determined by the movable mirror's amplitude, the light beam's spread angle in the optical interferometer, the movable mirror's tilt, and so on [Figure 3-7].
The wavenumber resolution is expressed by [Equation (3-6)] and improves as the movable mirror's amplitude increases.

$$\Delta v = \frac{1}{4L_1} \cdots\cdots\cdots\cdots (3\text{-}6)$$

Δv: wavenumber resolution
L_1 : amplitude

The effect of the light beam's spread angle is expressed by [Equation (3-7)].

$$\Delta v = \left(\frac{df}{2f}\right)^2 v \cdots\cdots\cdots\cdots (3\text{-}7)$$

df: diameter of input optical fiber
f : focal distance of incident lens
v : wavenumber [cm^{-1}]

[Figure 3-7] Lens and light beam

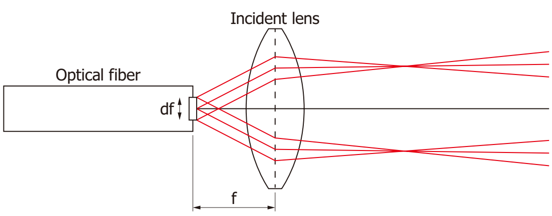

KACCC1015EA

Wavenumber resolution (unit: cm^{-1}) can be converted to spectral resolution (unit: nm) [Equation (3-8)]. The spectral resolution varies depending on the wavelength and degrades at longer wavelengths. [Figure 3-8] shows a typical example of the measured wavelength resolution.

$$\Delta\lambda = \left(\frac{1}{v} - \frac{1}{v + \Delta v}\right) \times 10^7 \cdots\cdots\cdots\cdots (3\text{-}8)$$

Δλ: spectral resolution

[Figure 3-8] Spectral resolution vs. wavelength (typical example, FWHM)

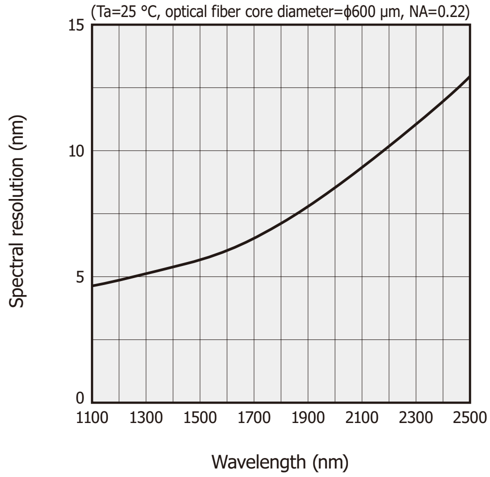

KACCB0602EA

[Table 3-2] shows the optical specifications of the FTIR engine.

[Table 3-2] Optical specifications

Parameter	Condition	Typ.	Unit
Optical input connector		SMA connector for optical fiber	-
Incident lens focal distance	λ=1150 nm	6.24	mm
Incident lens NA		0.4	-
Spectral resolution (FWHM)	λ=1532 nm	5.7	nm

Zero fill processing

One method of smoothing the acquired optical spectrum is zero fill processing [Figure 3-9]. This is a process of adding zeros at each end of the optical interference signal before the Fourier transform, which allows interpolation between points plotted after the Fourier transform. The resolution does not change in this case.

[Figure 3-9] Zero fill processing

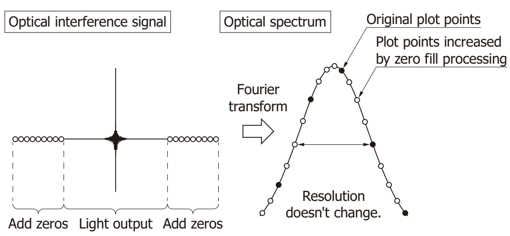

KACCC1016EA

3 - 3 Control circuit

The FPGA of the digital controller drives the movable mirror and controls the measurement timing. The movable mirror is driven when the built-in high voltage IC (HVIC) applies a square-wave drive voltage to the comb electrodes. The number of times the drive voltage is applied from when driving is started is counted.

The optical signals detected by the infrared interferometer and laser interferometer are amplified by the preamplifier and then converted to 16-bit digital signals by two A/D converters whose sampling timing is synchronized.

[Table 3-3] Electrical characteristics

Parameter	Typ.	Unit
A/D resolution	16	bit
A/D sampling rate	140	ns

The FTIR engine measurement starts when the drive voltage of the movable mirror is input. Data is acquired for the specified number of cycles, and the acquired optical signals are integrated in the FPGA [Figure 3-10]. The measurement data is defined by using the “0” or “1” of the least significant bit (LSB) according to the movable mirror’s vertical movement. The relationship between the movable mirror’s vertical movement and the “0” and “1” of the least significant bit changes each time drive start is set.

[Figure 3-10] Timing chart (Direction=0, Cycle=2)

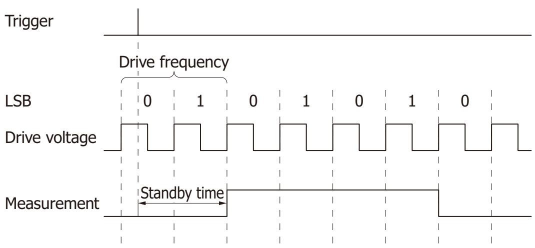

KACCC1017EB

The deviation between the phases of the movable mirror and the drive voltage decreases as the frequency approaches the resonant frequency, and the phases match at the resonant frequency. At the resonant frequency, the mirror amplitude changes drastically as shown in [Figure 3-2], making it difficult to control. The drive frequency under the FTIR engine’s recommended operating conditions is lower than the resonant frequency. As a result, a phase shift occurs between the movable mirror and the drive voltage [Figure 3-11]. Due to the phase shift, the digital data of the control circuit is valid up to the amplitude peak and invalid after the peak in [Figure 3-11].

[Figure 3-11] Amplitude and drive voltage of movable mirror (typical example)

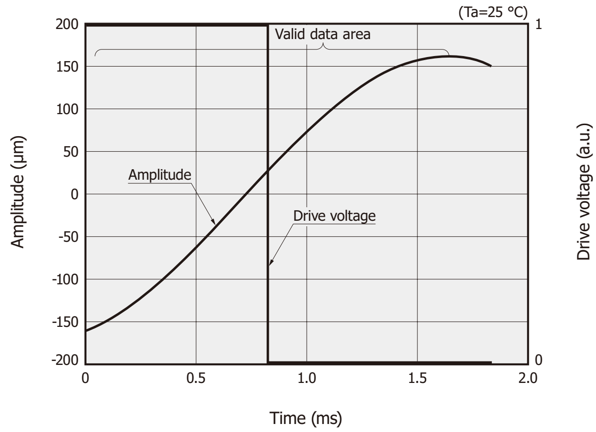

KACCB0663EA

[Figures 3-12] and [Figures 3-13] show the digital data measured by the infrared interferometer and laser interferometer.

[Figure 3-12] Digital data of infrared interferometer and laser interferometer (measurement example, Direction=0)

(a) Digital data

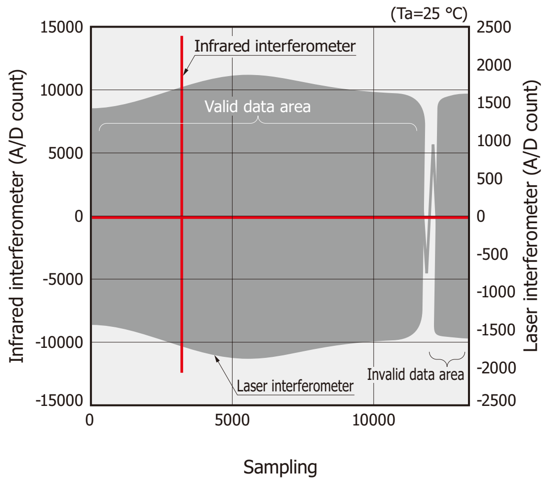

KACCB0604EA

(b) Enlarged view near zero optical path difference

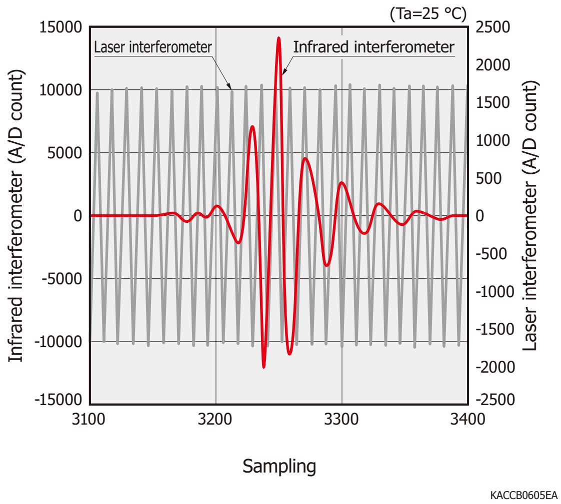

[Figure 3-13] Digital data of infrared interferometer and laser interferometer (measurement example, Direction=1)

(a) Digital data

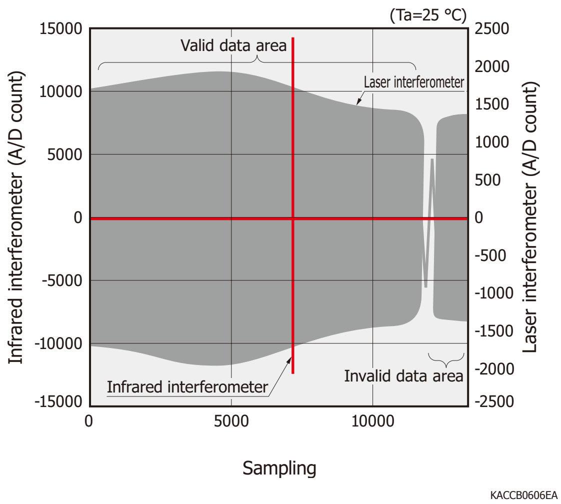

(b) Enlarged view near zero optical path difference

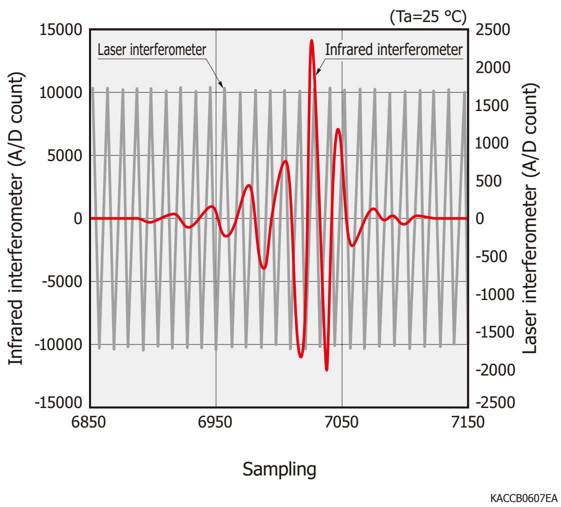

4. Characteristics

4 - 1 S/N

The FTIR engine's signal-to-noise ratio (S/N) is defined as the ratio between the maximum value of the optical spectrum and the effective noise value (RMS) when halogen light is incident. The light source output needs to be adjusted or an ND filter needs to be used to obtain an appropriate incident light level to prevent the FTIR engine's A/D converter from saturating. Since the FTIR engine uses 16-bit A/D converters, adjust the incident light level so that the optical interference signal is between 40000 and 64000 counts p-p. The incident light level needs to be adjusted for each product as the sensitivity differs by product [Figure 4-2].

[Figure 4-1] S/N measurement system

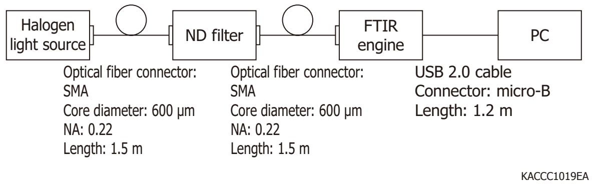

[Figure 4-2] Incident light level adjustment

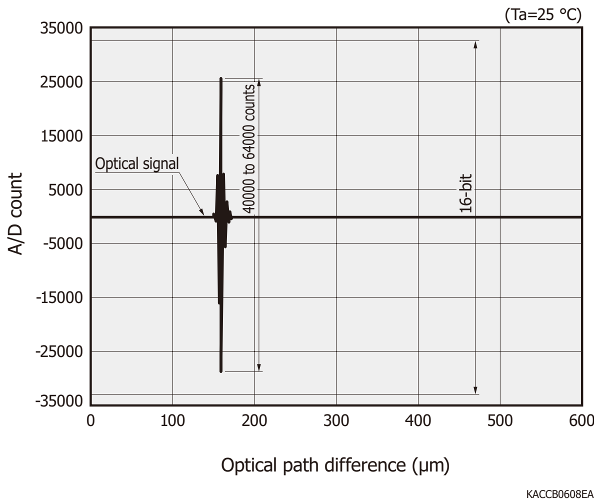

[Table 4-1] shows a typical example of the S/N characteristics in the measurement system of [Figure 4-1]. The S/N is 10000 or more at a gain setting between 1 and 4. The lower the gain, the lower the noise and the higher the S/N.

[Table 4-1] S/N characteristics (typical example, Ta=25 °C, halogen light source, optical fiber core diameter: 600 μm, NA: 0.22, integration count: 512, optical interference signal: approx. 40000 counts p-p)

Gain setting	Gain typ.	S/N typ.
0	Maximum	7500
1	High	15000
2	Middle	30000
3	Low	45000
4	Minimum	55000

[Figure 4-3] shows the optical spectrum when the light from the halogen light source is incident and the noise spectrum in the dark state. The optical spectrum near 1900 nm is the highest, and the S/N is also high.

[Figure 4-3] S/N characteristics (measurement example)

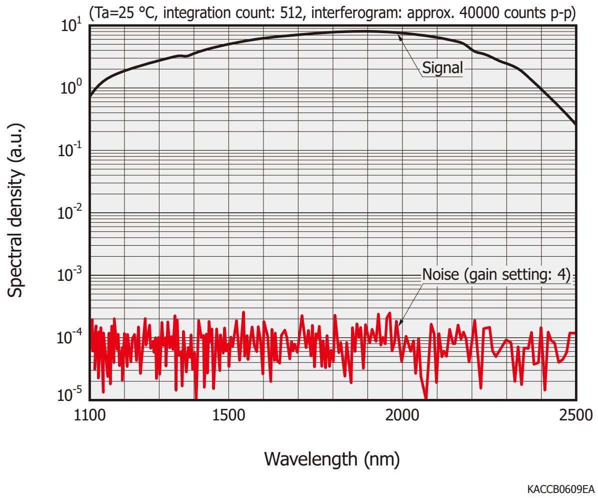

[Figure 4-4] shows the relationship between the effective value (RMS) of the noise and integration count. The noise is averaged by the movable mirror's integration count and is reduced to $1/\sqrt{N}$. Increasing the integration count increases the measurement time but increases the S/N.

[Figure 4-4] Noise characteristics (measurement example)

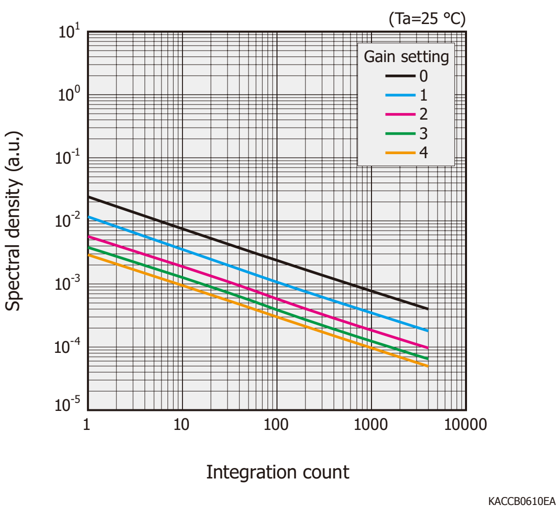

4 - 2 Effects of optical fiber transmission loss

The output optical spectrum changes depending on the transmission loss characteristics of the optical fiber connected to the FTIR engine. A quartz fiber has a loss depending on the length of the optical fiber in the wavelength range longer than 2.1 μm. For this reason, a short optical fiber or fluoride fiber is recommended. [Figure 4-6] shows the optical spectra when a fluoride fiber and quartz fibers of different lengths are used.

[Figure 4-5] Effects of optical fiber transmission loss

(a) Measurement system

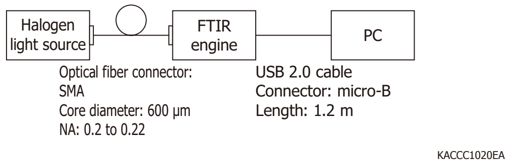

(b) Optical spectra (measurement example)

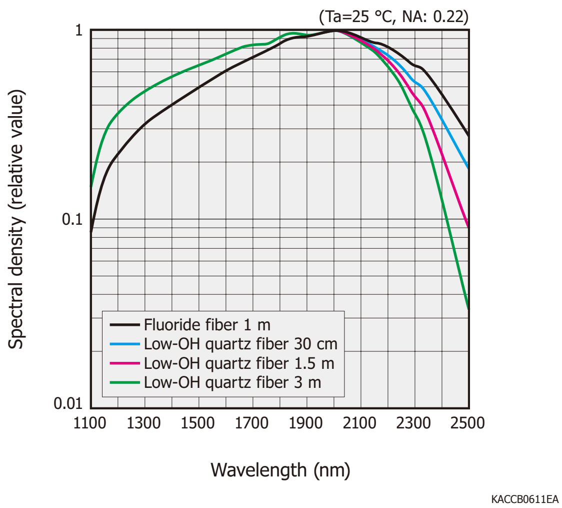

4 - 3 Wavelength temperature dependence

[Figure 4-7] shows the temperature characteristics of the peak wavelength and wavelength resolution (FWHM) of the laser spectrum measured by the FTIR engine in the measurement system shown in [Figure 4-6]. In this setup, a laser light (1532.8 nm) is input through an optical fiber, and the FTIR engine is placed in a constant temperature chamber. The FTIR engine is installed on a vibration isolation table to mitigate the effects of vibration in the constant temperature chamber.

[Figure 4-6] System for measuring temperature characteristics of wavelength accuracy and wavelength resolution

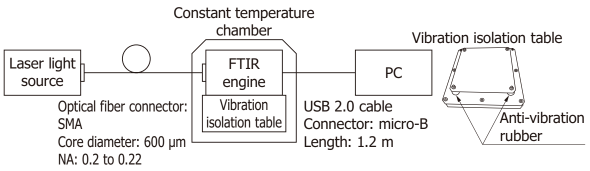

[Figure 4-7] Wavelength temperature dependence (typical example)

(a) Peak wavelength

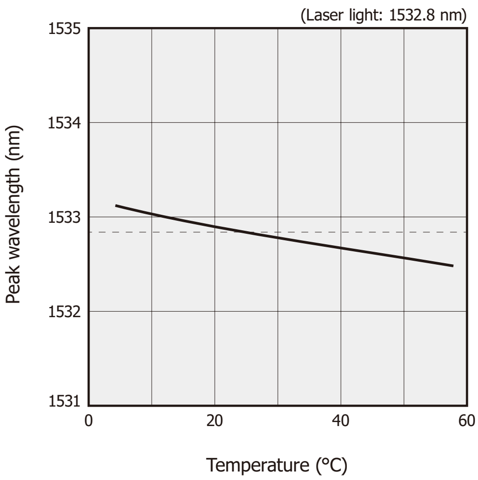

(b) Spectral resolution

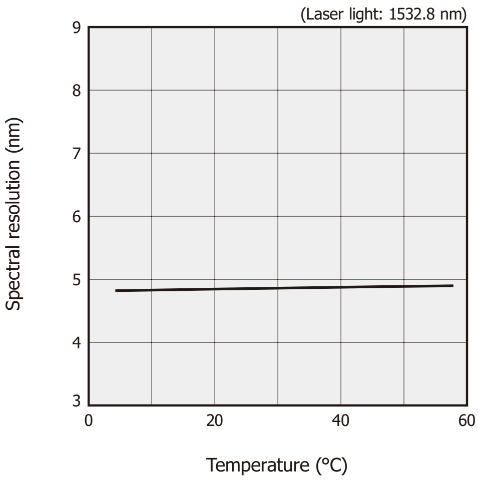

The FTIR engine's wavelength temperature dependence depends on the oscillation wavelength of the VCSEL used to monitor the movable mirror. Since the VCSEL changes its oscillation wavelength depending on temperature, the wavelength accuracy measured by the FTIR engine has temperature characteristics. In [Figure 4-7], the temperature measured by the thermistor in the FTIR engine when the temperature of the constant temperature chamber is changed is shown on the horizontal axis. The temperature inside the FTIR engine rises by about 5 °C due to the heat generated by the circuit driven by the FTIR engine. The peak wavelength of the laser spectrum detected by the FTIR engine shifts with temperature, and the wavelength temperature dependence is ±0.06 nm/°C or less. Note that the wavelength resolution (FWHM) is almost constant even when the temperature changes.

5. Measurement example

Measurement methods for near-infrared spectroscopy using the FTIR engine include measurement methods such as transmittance measurement and diffuse reflection measurement [Figure 5-1]. Please refer to the following documents for the principles of each measurement method and measurement examples.

Catalogs

- Product information / FTIR engine measurement examples
- Product information / Pharmaceutical analysis using diffuse reflection light source and near infrared spectrometers

https://www.hamamatsu.com/eu/en/product/optical-sensors/spectrometers/mini-spectrometer/related_documents.html

[Figure 5-1] Connection example

(a) Transmittance measurement

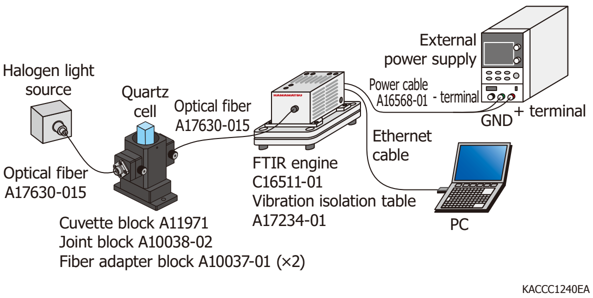

(b) Diffuse reflection measurement

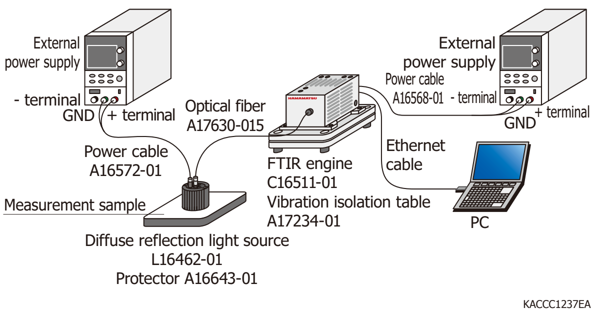

6. Related products

Various accessories (sold separately) are available for accurate and stable measurement shown in Figure 5-1.

Vibration isolation table

Since the FTIR engine is easily affected by vibration, a vibration isolation table is used to ensure stable measurements. Anti-vibration gels are contained in the vibration isolation table to mitigate the effects of vibration. Mounting screws are used to secure the FTIR engine to the vibration isolation table.

[Figure 6-1] Vibration isolation table with FTIR engine mounted

(a) Vibration isolation table A15835-01 + C15511-01

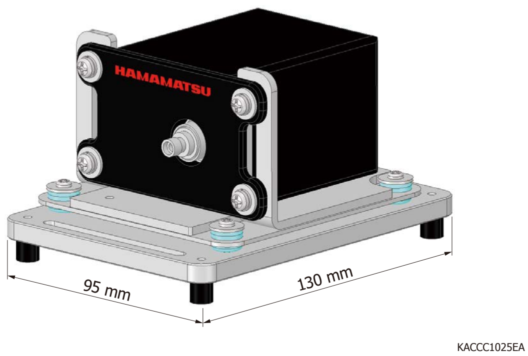

(b) Vibration isolation table A17234-01 + C16511-01

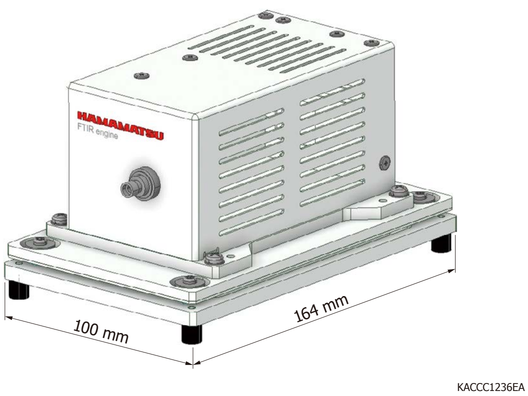

Diffuse reflection light source L16462-01

This is a lamp module for measuring diffuse reflection in near-infrared spectrophotometry. The lamp irradiates the sample with light and the light diffused and reflected within the sample is guided to the fiber. Spectrophotometry is performed by connecting to a near-infrared spectrometer or the like.

Response range	Size	Service life
400 to 2500 nm	ϕ28.0 × 35.5 mm	7000 hr (average)

[Figure 6-2] Diffuse reflection light source L16462-01

Protector A16643-01

This accessory is used to suppress heat generation and temperature rise of the diffuse reflection light source L16462-01.

Dimensions	Weight
ϕ46 × 35.5 mm	Approx. 55 g

Optical fiber cable A17630-015

Connector	Specification
SMA on each end	600 μm core, NA=0.22, Low-OH optical fiber, length=1500 mm Metal covering, With CPS (Cladding Power Stripper)

Power cable

· For C16511-01

Type no.	Connector	Specification
A16568-01	HR10-7P-4P (73)	Length: 2 m, One end: lead wire soldering, Wire: AWG26

· For L16462-01

Type no.	Connector	Specification
A16572-01	FGG.00.302CLAD35	Length: 1.5 m, One end: lead wire soldering, Wire: AWG26

Cuvette block A11971

This is a small dark box specifically designed for cuvettes with an optical path length of 10 mm.

Effective optical path diameter	Applicable cuvette size		Weight
	Optical path length	Dimensions	
8 mm	10 mm	□12.5 × 56 (H) mm	Approx. 200 g (Including the base)

Joint block A10038-02

This is a joint block for connecting one optical block to another.

Type	Effective optical path diameter	Weight
Female to female	10 mm	Approx. 25 g

Fiber adapter block A10037-01

This is a block that can connect optical fiber cables with SMA connectors. The lens assembled in the block collimates the light spread from the optical fiber.

Recommended wavelength	Connector	Focal distance	Weight
Visible region	SMA	10 mm	Approx. 17 g

Related information
www.hamamatsu.com/sp/ssd/doc_en.html

Precautions
· Disclaimer

Information described in this material is current as of April 2025.
Product specifications are subject to change without prior notice due to improvements or other reasons. This document has been carefully prepared and the information contained is believed to be accurate. In rare cases, however, there may be inaccuracies such as text errors. Before using these products, always contact us for the delivery specification sheet to check the latest specifications.
The product warranty is valid for one year after delivery and is limited to product repair or replacement for defects discovered and reported to us within that one year period. However, even if within the warranty period we accept absolutely no liability for any loss caused by natural disasters or improper product use.
Copying or reprinting the contents described in this material in whole or in part is prohibited without our prior permission.

HAMAMATSU

www.hamamatsu.com

Optical Semiconductor Sales, HAMAMATSU PHOTONICS K.K.
1126-1 Ichino-cho, Chuo-ku, Hamamatsu City, Shizuoka Pref., 435-8558 Japan, Telephone: (81)53-434-3311, Fax: (81)53-434-5184
U.S.A.: HAMAMATSU CORPORATION: 360 Foothill Road, Bridgewater, NJ 08807, U.S.A., Telephone: (1)908 231 0960, Fax: (1)908 231 1218
Germany: HAMAMATSU PHOTONICS DEUTSCHLAND GMBH: Arzbergerstr. 10, 82211 Herrsching am Ammersee, Germany, Telephone: (49)8152 375 0, Fax: (49)8152 265 8 E mail: info@hamamatsu.de
France: HAMAMATSU PHOTONICS FRANCE S.A.R.L.: 19 Rue du Saule Trapu, Parc du Moulin de Massy, 91882 Massy Cedex, France, Telephone: (33)1 69 53 71 00, Fax: (33)1 69 53 71 10 E mail: infos@hamamatsu.fr
United Kingdom: HAMAMATSU PHOTONICS UK LIMITED: 2 Howard Court,10 Tewin Road, Welwyn Garden City, Hertfordshire, AL7 1BW, UK, Telephone: (44)1707 294888, Fax: (44)1707 325777 E mail: info@hamamatsu.co.uk
North Europe: HAMAMATSU PHOTONICS NORDEN AB: Torshamnsgatan 35, 16440 Kista, Sweden, Telephone: (46)8 509 031 00, Fax: (46)8 509 031 01 E mail: info@hamamatsu.se
Italy: HAMAMATSU PHOTONICS ITALIA S.R.L.: Strada della Moia, 1 int. 6 20044 Arese (Milano), Italy, Telephone: (39)02 93 58 17 33, Fax: (39)02 93 58 17 41 E mail: info@hamamatsu.it
China: HAMAMATSU PHOTONICS (CHINA) CO., LTD.: 1201, Tower B, Jiaming Center, 27 Dongsanhuan Beilu, Chaoyang District, 100020 Beijing, P.R. China, Telephone: (86)10 6586 6006, Fax: (86)10 6586 2866 E mail: hpc@hamamatsu.com.cn
Taiwan: HAMAMATSU PHOTONICS TAIWAN CO., LTD.: 13F 1, No.101, Section 2, Gongdao 5th Road, East Dist., Hsinchu City, 300046, Taiwan(R.O.C) Telephone: (886)3 659 0080, Fax: (886)3 659 0081 E mail: info@hamamatsu.com.tw
Korea: HAMAMATSU PHOTONICS KOREA CO., LTD.: A 912, 167, Songpa daero, Seoul, 05855, Korea, Telephone: (82)2 2054 8202, Fax: (82)2 2054 8207 E mail: sales@hpkr.co.kr

Cat. No. KACC9012E04 Apr. 2025 DN